ISSN 1027-4510, Journal of Surface Investigation. X-ray, Synchrotron and Neutron Techniques, 2012, Vol. 6, No. 2, pp. 271–276. © Pleiades Publishing, Ltd., 2012.
Original Russian Text © Yu.P. Kunashenko, 2012, published in Poverkhnost'. Rentgenovskie, Sinkhrotronnye i Neitronnye Issledovaniya, 2012, No. 3, pp. 89–95.

Schwinger Scattering of Fast Neutrons in Crystals

Yu. P. Kunashenko[a, b]

[a] *Tomsk Polytechnic National Research University, pr. Lenina 30, Tomsk, 634050 Russia*
[b] *Tomsk State Pedagogical University, ul. Kievskaya 60, Tomsk 634061 Russia*
e-mail: kunashenko@tpu.ru

Received March 17, 2011

Abstract—The coherent effects emerging during fast neutron passage through oriented crystals have been investigated. It has been demonstrated that the cross section of coherent Schwinger neutron scattering in a crystal has maxima at specific entry angles and neutron energies. The effect of energy divergence and angular dispersion in a neutron beam on the coherent peak value has been examined.

DOI: 10.1134/S1027451012030159

INTRODUCTION

It is generally known that coherent effects emerge during the passage of fast charged particles through oriented crystals due to the periodical location of atoms in crystals. In this case the scattering amplitudes on individual crystal atoms are phase-added, thus producing an interference factor in the scattering cross section that results in bright coherent maxima at the coincidence of the transferred momentum with one of the reciprocal lattice vectors [1]. Channeling comprises another effect accompanying the passage of fast charged particles through oriented crystals. During entry into a crystal at a small angle relative to the axis (plane), particle motion is controlled by continuous potentials of the crystal axes or planes [2].

A neutron is a neutral particle, but, as was shown by Schwinger [3], it can be scattered in an atom's electrical field due to the presence of spin (and, therefore, of magnetic moment). Schwinger neutron scattering was discovered in 1956 [4]. The paper devoted to the 50th anniversary of this discovery [5] reviewed theoretical and experimental works on this subject and described possible new experiments concerning neutron scattering by the electrical fields of atoms.

Similarly to the coherent effect upon the scattering of fast charged particles in oriented crystals, one could expect the emergence of this effect in crystals, in addition to regular nucleus scattering. For the first time, the existence of coherent effects in Schwinger neutron scattering was described in [6, 7]. The only experiment concerned with measuring the cross section of Schwinger neutron scattering in a germanium crystal was carried out in [8]. However, the results of theoretical works [6, 7] do not agree with each other and also poorly agree with the experimental results in [8]. The objective of the present work was to carry out more detailed calculations of the coherent Schwinger scattering of fast neutrons in a crystal to determine the optimal conditions for experimental studies of this phenomenon.

We applied an approach similar to that of the authors of [7]. A new feature of our approach is to take into account the incoherent contribution to the scattering cross section, which was not examined in [6, 7]. It is generally known that the value of the incoherent contribution to the cross section is comparable to that for the majority of coherent processes [1]. Besides this, our approach allows the incoherent Schwinger scattering of fast neutrons in a crystal at any (axis and plane) crystal orientation to be investigated. For the first time this approach was applied in [9].

SCHWINGER SCATTERING OF FAST NEUTRONS IN CRYSTALS

The cross section of Schwinger neutron scattering on an individual atom can be written as [3]

$$\frac{d\sigma_1}{d\Omega} = \frac{\gamma_n^2}{4}\left(\frac{e^2}{M}\right)^2 [Z - F(q)]^2 \cot^2\frac{\theta}{2}. \quad (1)$$

Here q is the transferred momentum; Z is the atomic number; $F(q)$ is the atomic form factor; M is the neutron weight; γ_n is the neutron magnetic moment in $e\hbar/2Mc$, units; θ is the neutron scattering angle. The units $\hbar = c = 1$ are used.

Let us select the screened potential of an atom as

$$V(r) = \frac{Ze}{r}\exp(-r/R_s), \quad (2)$$

then

$$\frac{d\sigma_1}{d\Omega} = \frac{\gamma_n^2}{4}\left(\frac{Ze^2}{M}\right)^2 \frac{q^4}{\left(q^2 + R_s^2\right)^2}\cot^2\frac{\theta}{2}, \quad (3)$$

where R_s is the atom screening radius, $q^2 = 2p^2(1 - \cos\theta) = 4p^2\sin^2\frac{\theta}{2}$ is the transferred momentum square, and p is the initial neutron momentum.

The cross section (3) has a maximum at the scattering angle

$$\theta_1 = \arccos\left(\frac{2E_k^2R_s^2}{1 + 2E_k^2R_s^2}\right), \tag{4}$$

where E_k is the neutron kinetic energy. The cross-section maximal value is equal to

$$\frac{d\sigma_1(\theta_1,\gamma)}{d\Omega} = Z^2e^2\gamma_n^2\frac{E_k^2R_s^4}{1 + 4E_k^2R_s^2}. \tag{5}$$

In a crystal the cross section is represented as a sum of the coherent $d\sigma_{\text{coh}}$ and incoherent $d\sigma_{\text{incoh}}$ contributions:

$$d\sigma_{\text{cr}} = d\sigma_{\text{coh}} + d\sigma_{\text{incoh}}; \tag{6}$$

$$d\sigma_{\text{coh}} = I(\mathbf{q})|S(\mathbf{q})|^2\exp\left(-q^2\overline{u^2}\right)d\sigma_1; \tag{7}$$

$$d\sigma_{\text{incoh}} = N_{\text{tot}}\left[1 - \exp\left(-q^2\overline{u^2}\right)\right]d\sigma_1. \tag{8}$$

Here $I(\mathbf{q})$ is the interference factor responsible for the emergence of incoherent effects; $\exp\left(-q^2\overline{u^2}\right)$ is the Debye–Waller factor, taking into account the thermal vibrations of crystal atoms; $\overline{u^2}$ is the mean square deviation of atoms from the equilibrium position; $N_{\text{tot}} = N_XN_YN_Z$ is the total number of atoms in the crystal; $S(\mathbf{q})$ is the structural factor. In the case of a thin crystal, when $N_X \gg 1$, $N_Y \gg 1$, and $N_Z \ll N_X$, N_Y in the reference system of which the OZ axis is directed along the crystal ⟨100⟩ axis, the interference factor can be written as

$$I(\mathbf{q}') = N_XN_Y\frac{(2\pi)^2}{d_yd_x}\sum_{n,l}\delta\left(q'_x - g_xn\right)\delta\left(q'_y - g_ym\right) \times \frac{\sin^2\left(\frac{1}{2}N_Zq'_zd_z\right)}{\sin^2\left(\frac{1}{2}q'_zd_z\right)}. \tag{9}$$

Here $\mathbf{q}'$ is the transferred momentum; N_X, N_Y, and N_Z are the number of crystal atoms in the X', Y' and Z' directions, respectively; $g_x = 2\pi/a_x$, $g_y = 2\pi/a_y$ @@@@@@@@@@@@ X'- Y', a_x, a_y are the lattice constants.

1 Let us rewrite the cross section of Schwinger neutron scattering in terms of the transferred momentum $\mathbf{q}$. If the OZ axis is selected in the direction of the initial neutron momentum p, then

$$q_x = p\cos\varphi\sin\theta; \quad q_y = p\sin\varphi\sin\theta. \tag{10}$$

Here θ and φ are the scattering angles, for which the following formula can be easily obtained:

$$\theta(q_x,q_y) = \arcsin\left(\frac{\sqrt{q_x^2 + q_y^2}}{p}\right), \quad \varphi(q_x,q_y) = \arccos\left(\frac{q_x}{\sqrt{q_x^2 + q_y^2}}\right). \tag{11}$$

For the solid angle element $d\Omega$, we obtain

$$d\Omega = \frac{dq_ydq_x}{p\sqrt{p^2 - q_x^2 - q_y^2}}. \tag{12}$$

In these variables the Schwinger neutron scattering 1
cross section will be written as

$$d\sigma = \frac{\gamma_n^2}{4}\left(\frac{Ze^2}{M}\right)^2\frac{q^4}{\left(q^2 + R_s^2\right)^2}\left(\frac{p + \sqrt{p^2 - q_x^2 - q_y^2}}{p - \sqrt{p^2 - q_x^2 - q_y^2}}\right) \times \frac{dq_xdq_y}{p\sqrt{p^2 - q_x^2 - q_y^2}}. \tag{13}$$

The formula (13) is expressed in a coordinate system related to the initial neutron momentum, whereas the formula for the interference factor is written in a system related to the crystal. The relationship between these coordinate systems is provided by the formulas [1]

$$\left.\begin{aligned} q'_x &= q_z\sin\Psi - (q_x\sin\Phi - q_y\cos\Phi)\cos\Psi, \\ q'_y &= q_x\cos\Phi + q_y\sin\Phi, \\ q'_z &= q_z\cos\Psi - (q_x\sin\Phi - q_y\cos\Phi)\sin\Psi. \end{aligned}\right\}, \tag{14}$$

where Ψ is the neutron entry angle counted from the crystal ⟨100⟩ axis, and Φ is the neutron entry angle in the plane perpendicular to the axis (the polar angle; the angle between the neutron momentum and crystallographic plane (100)). The relationship between the coordinate systems is shown in Fig. 1.

If the experiment detects neutrons scattered in a certain angle range, for example, at the solid angle $\Delta\Omega_1$ ($\vartheta_1 = 0 - \Theta_{\max}$, $\varphi_1 = 0 - 2\pi$), one should integrate the cross section for coherent Schwinger neutron scat- 1
tering over the angles:

$$\sigma_{\text{cr}} = \int_{\Delta\Omega}\frac{d\sigma_{\text{cr}}}{d\Omega'}d\Omega' = \sigma_{\text{coh}} + \sigma_{\text{incoh}} = \int_{\Delta\Omega}\frac{d\sigma_{\text{coh}}}{d\Omega'}d\Omega' + \int_{\Delta\Omega}\frac{d\sigma_{\text{incoh}}}{d\Omega}d\Omega = \int_0^{q_{\perp\max}}\frac{d\sigma_{\text{coh}}}{dq'_xdq'_y}\left(q'_xq'_y\right)dq'_xdq'_y + \int_0^{2\pi}d\varphi\int_0^{\Theta_{\max}}\sin\theta d\theta\frac{d\sigma_{\text{incoh}}}{d\Omega}(\theta,\varphi). \tag{15}$$

Here $\Theta_{\max}$ is the maximal neutron scattering angle relative to the initial momentum vector (the angle size of

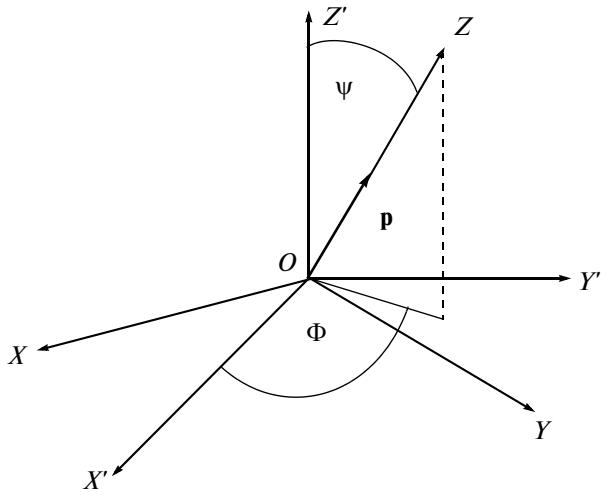

Fig. 1. The coordinate system $X'Y'Z'$ is related to crystal axes: the $O'Z'$ coincides with the crystallographic axis ⟨100⟩, the plane $Z'O'Y'$ coincides with the crystallographic plane (100). The coordinate system XYZ is related to the initial neutron momentum **p**, which is directed along the initial neutron momentum **p**; ψ is the neutron entry angle relative to the $O'Z'$ axis; Φ is the neutron entry angle in the $X'O'Y'$ plane (the polar angle; the angle between the neutron momentum and the crystallographic plane (100)).

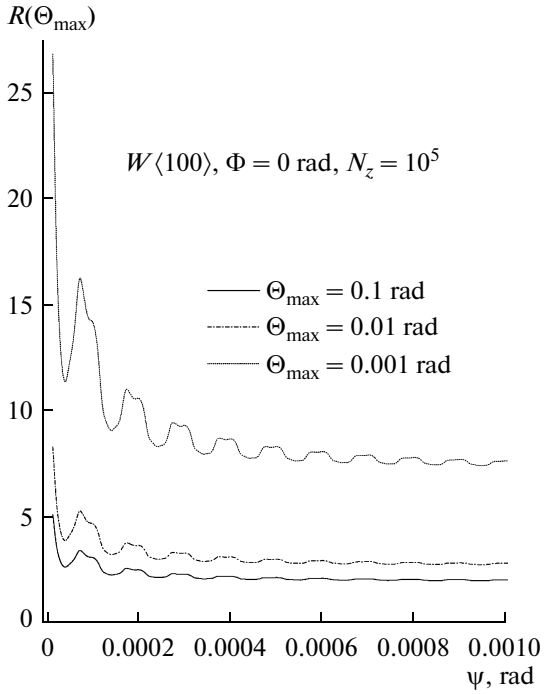

Fig. 2. The dependence of the relation $R(\Theta_{max})$ on the neutron entry angle Ψ relative to the crystal axis ⟨100⟩ (angle Φ = 0) for different collimation angles: Θ_{max} = 0.1 rad (solid line), Θ_{max} = 0.01 rad (dash-and-dot line), Θ_{max} = 0.001 rad (dashed line). The crystal W ⟨100⟩, $\sqrt{\overline{u^2}} = 0.022$ Å; the crystal temperature $T = 0$ K; $N_z = 10^5$.

the collimator); $q_{\perp max}$ is the maximal value of the transferred momentum in the plane perpendicular to the crystal ⟨100⟩ axis. The value of $q_{\perp max}$ is determined by the value of the Θ_{max} angle: $q^2_{\perp max} = p^2\sin^2\Theta_{max}$.

After substitution of (7), (9), (13) into (15) and integration of the cross-section's coherent part, one obtains

$$\sigma_{coh}(\Theta_{max}) = \frac{\gamma_n^2}{4}\left(\frac{Ze^2}{M}\right)^2 N_x N_y \frac{(2\pi)^2}{d_y d_x} \times \sum_{n,m}\left\{\frac{\left(q'^2_{\perp nm} + q'^2_{znm}\right)^2}{\left(q'^2_{\perp nm} + q'^2_{znm} + R^{-2}\right)^2}\left(\frac{p + \sqrt{p^2 - q'^2_{\perp nm}}}{p - \sqrt{p^2 - q'^2_{\perp nm}}}\right)\right. \times \frac{\exp\left(-\left(q'^2_{\perp nm} + q'^2_{znm}\right)\overline{u^2}\right)}{p\sqrt{p^2 - q'^2_{\perp nm}}} \left.\times \frac{\sin^2\left(\frac{1}{2}N_z q'^2_{znm} d_z\right)}{\sin^2\left(\frac{1}{2}q'_{znm} d_z\right)}\left|S\left(q'_{\perp nm}, q'_{znm}\right)\right|^2\right\}. \quad (16)$$

Here the following notation is used: $q'^2_{\perp nm} = g_x^2 n^2 + g_y^2 m^2$, $q'_{znm} = p - \sqrt{p^2 - q'^2_{\perp nm}}$.

Summation in (16) is carried out taking into account the condition $q'^2_{\perp nm} \le q^2_{\perp max}$. As follows from (16), the coherent peaks emerge when the condition

$$\frac{1}{2}q'_{znm} d_z = \pi k,\ k = 1, 2, 3, \ldots .$$

is fulfilled. Integration of the cross-section's incoherent part was performed numerically:

$$\sigma_{incoh}(\Theta_{max}) = N_{tot}\int_{\Delta\Omega}\left[1 - \exp\left(-q^2(\theta,\varphi)\overline{u^2}\right)\right]\frac{d\sigma_1}{d\Omega}(\theta,\varphi)d\Omega. \quad (17)$$

Further calculations were performed using the formulas (16), (17).

RESULTS OF NUMERICAL CALCULATIONS

It is convenient to introduce the ratio of the Schwinger neutron scattering cross section in a crystal to that in an amorphous target containing the same number of atoms:

$$R(\Theta_{max}) = \frac{\sigma_{coh}(\Theta_{max}) + \sigma_{incoh}(\Theta_{max})}{N_{tot}\sigma_1(\Theta_{max})}.$$

Figure 2 shows the dependence of the ratio $R(\Theta_{max})$ on the neutron entry angle Ψ relative to the crystal axis ⟨100⟩ (angle Φ = 0). For different collimation angles:

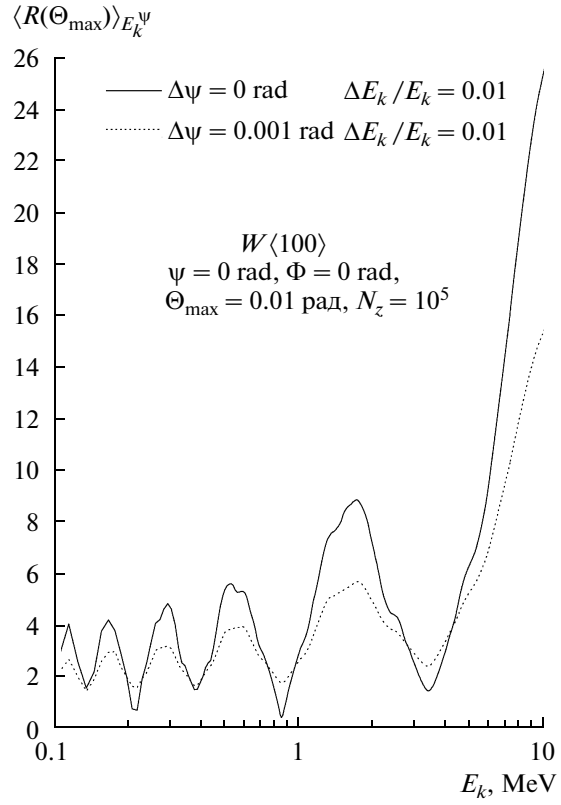

Fig. 3. The dependence of the relation $\langle R(\Theta_{max})\rangle_{E_k\Psi}$ on the neutron kinetic energy; the neutron entry angles are $\Phi = 0$ and $\Phi = 0$; the collimation angle is $\Theta_{max} = 0.001$ rad. The energy ($\Delta E_k/E_k$ and angle $\Delta\psi = 0.001$ rad) dispersions are taken into account (dashed line); solid line shows the data excluding this. Other parameters are similar to Fig. 2.

$\Theta_{max} = 0.1$ rad (solid line), $\Theta_{max} = 0.01$ rad (dash-and-dot line), $\Theta_{max} = 0.001$ rad (dashed line). The neutron kinetic energy E_k = 1.5 MeV; the crystal $W\langle 100\rangle$, $\sqrt{\overline{u}^2} = 0.022$ Å; the temperature of the crystal $T = 0$ K; $N_z = 10^5$. As seen from the figure, the coherent effect's brightness increases with an increase in the collimation angle.

In real experiments neutron beams are characterized by energy and angular divergence. That is why the obtained results should be averaged over the energy and angular dispersion. Since the incoherent contribution to the cross section and the Schwinger neutron scattering cross section in an amorphous target do not depend on the neutron angles of entry into a crystal and change gradually along with variation in the neutron energy, we limited ourselves to averaging only the coherent contribution to the cross section:

$$\langle R(\Theta_{max})\rangle_{E_k(\Psi)} = \frac{\langle\sigma_{coh}(\Theta_{max})\rangle_{T(\Psi)} + \sigma_{incoh}(\Theta_{max})}{N_{tot}\sigma_1(\Theta_{max})}.$$

Here the coherent contribution to the Schwinger neutron scattering cross section averaged over the energy dispersion (ΔE_k is the dispersion width) is equal to

$$\langle\sigma_{coh}(\Theta_{max})\rangle_{E_k} = \frac{1}{\Delta E_k}\int_{E_k-\Delta E_k}^{E_k+\Delta E_k}\sigma_{coh}(\Theta_{max})\,dE_k.$$

The contribution averaged over angular dispersion with the width $\Delta\Psi$ will be written as

$$\langle\sigma_{coh}(\Theta_{max})\rangle_{\Psi} = \frac{1}{\Delta\Psi}\int_{\Psi-\Delta\Psi}^{\Psi+\Delta\Psi}\sigma_{coh}(\Theta_{max})\,d\Psi,$$

whereas the contribution averaged simultaneously over the energy (ΔE_k) and angle ($\Delta\Psi$) dispersion is equal to

$$\langle\sigma_{coh}(\Theta_{max})\rangle_{E_k\Psi} = \frac{1}{\Delta\Psi}\frac{1}{\Delta E_k}\int_{E_k-\Delta E_k}^{E_k+\Delta E_k}\int_{\Psi-\Delta\Psi}^{\Psi+\Delta\Psi}\sigma_{coh}(\Theta_{max})\,d\Psi\,dE_k.$$

Figure 3 shows the dependence of the relation $\langle R(\Theta_{max})\rangle_{E_k\Psi}$ on the neutron kinetic energy E_k. The neutron entry angles are $\Psi = 0$ and $\Phi = 0$; the collimation angle is $\Theta_{max} = 0.01$ rad. In Fig. 3, dots reflect the results of the calculation taking into account averaging, and the solid line shows data excluding the dispersion. Other parameters are similar to Fig. 2. As seen from Fig. 3, in the case of the energy dependence of the Schwinger neutron scattering cross section, the effect of energy and angular dispersion appears to be weak, the coherent effect remains distinctly expressed, while the values of the coherent peaks undergo an approximately twofold decrease.

Figures 4 and 5 show the dependence of the relations $\langle R(\Theta_{max})\rangle_{E_k}$(A) and $\langle R(\Theta_{max})\rangle_{\Psi}$ on the neutron entry angle Φ relative to the crystal $\langle 100\rangle$ axis. The angle is $\Phi = 0$, the collimation angle is $\Theta_{max} = 0.001$ rad (Fig. 4) and $\Theta_{max} = 0.01$ rad (Fig. 5). In Fig. 5a, the angular dispersion $\Delta\Psi = 0.001$ rad (dashed line) is taken into account. The results excluding dispersion are shown by a solid line. Figure 5b takes into account the energy dispersion: $\Delta E_k/E_k = 0.1$ is shown by dots; $\Delta E_k/E_k = 0.5$ is shown by a dashed line; excluding the dispersion is shown by a solid line. The other parameters are similar to Fig. 2.

As seen from the figures, small angular dispersion of the neutron beam results in a significant reduction and variation in the character of the orientation dependence. Instead of ten narrow and bright coherent peaks, there emerges one broad, diffuse peak. The peak size reduces approximately threefold as compared to the brightest peak in the absence of angular dispersion.

On the other hand, the energy dispersion in the neutron beam virtually has no influence on the coherent effect. For the energy dispersion $\Delta E_k/E_k =$

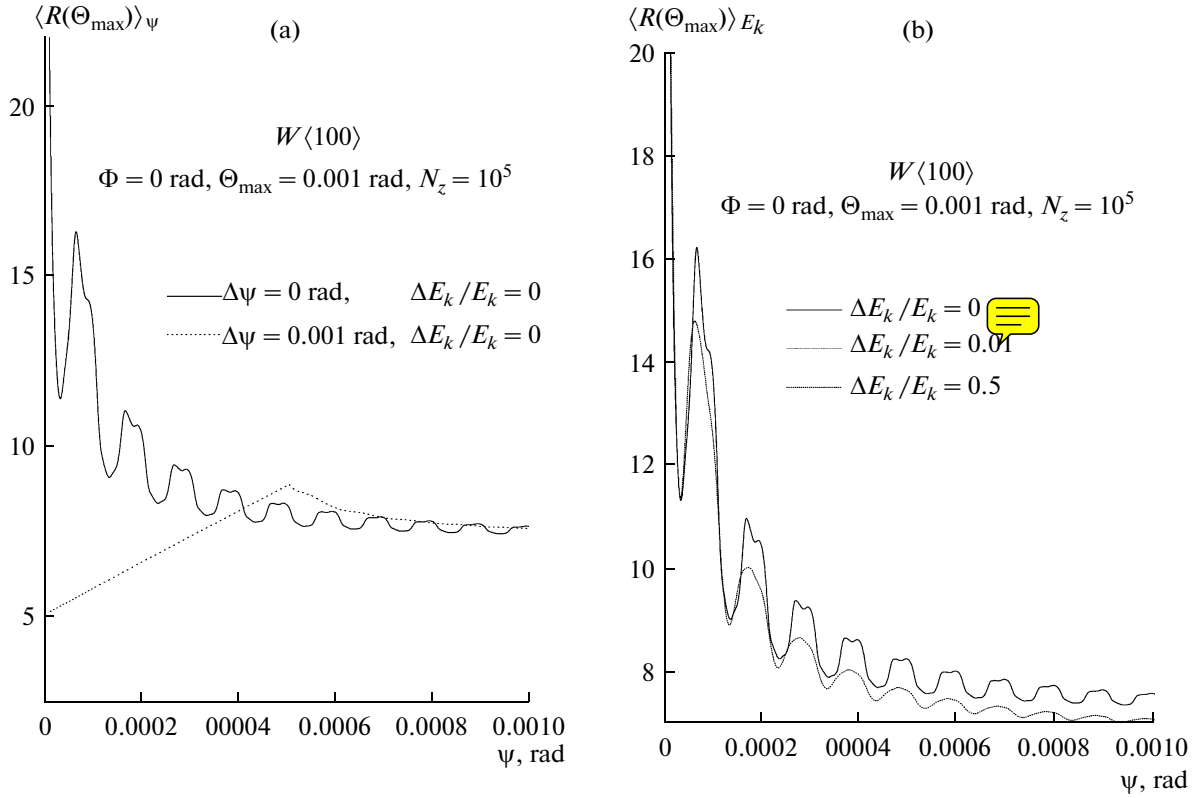

Fig. 4. The dependence of the relations $\langle R(\Theta_{max})\rangle_{\Psi}$ and $\langle R(\Theta_{max})\rangle_{E_k}$ (b) on the neutron entry angle Ψ relative to the crystal axis ⟨100⟩, the angle Φ = 0 The collimation angle $\Theta_{max} = 0.001$ rad. The angular dispersion $\Delta\psi = 0.001$ rad (dashed line) is taken into account. The results excluding the dispersion are shown by the solid line (a). The energy dispersion is taken into account: $\Delta E_k/E_k = 0.1$ is shown by the bold dashed line; $\Delta E_k/E_k = 0.5$ is shown by the light dashed line; excluding the dispersion is shown by the solid line (b). At $\Delta E_k/E_k = 0.1$ and $\Delta E_k/E_k = 0$ the results of the calculation practically coincide and the curves merge. The other parameters are similar to Fig. 2.

0.5, the coherent effect remains sufficiently bright. At the values $\Delta E_k/E_k = 0.1$ and $\Delta E_k/E_k = 0$, the results of the calculation virtually coincide: in Fig. 4b ($\Theta_{max} = 0.001$ rad), the curves corresponding to these values become the same.

As seen from Figs. 2, 4, and 5, the cross section has sharp coherent peaks at specific neutron entry angles. With a decrease in the collimation angle, the brightness of the coherent peak increases. Such an effect is observed during coherent pair photoproduction under the tight collimation conditions of the formed electron and positron [10, 11].

CONCLUSIONS

The performed studies have demonstrated the following:

(1) In a crystal the coherent effect results in a substantial increase in the Schwinger neutron scattering cross section at certain neutron energies and entry angles.

(2) The value of the coherent peak depends on the collimator angle sizes.

(3) The effect of energy dispersion and angular divergence in the initial neutron beam on the energy dependence of the Schwinger neutron scattering cross section in a crystal does not occur.

(4) Angular dispersion results in a substantial decrease and character change in the orientation dependence, whereas energy dispersion is practically negligible.

The Schwinger scattering cross section on the axis $\langle 1\bar{1}0\rangle$ of a Ge crystal with the thickness 56 mm was studied experimentally [8]. Such a crystal is too thick to study coherent effects. The value of the coherent effect was approximately $(\sigma_{max} - \sigma_{min})/\sigma_{min} \approx 0.01$, which is much lower than theoretical predictions [6, 7, 9]. This discrepancy between theory and experiment is, most probably, explained by angular divergence in the initial neutron beam.

It is further assumed that the nuclear interaction should be taken into account along with the Schwinger electromagnetic interaction. In this case, as was shown in [3], the neutron scattering cross section consists of three components: electromagnetic, nuclear, and that

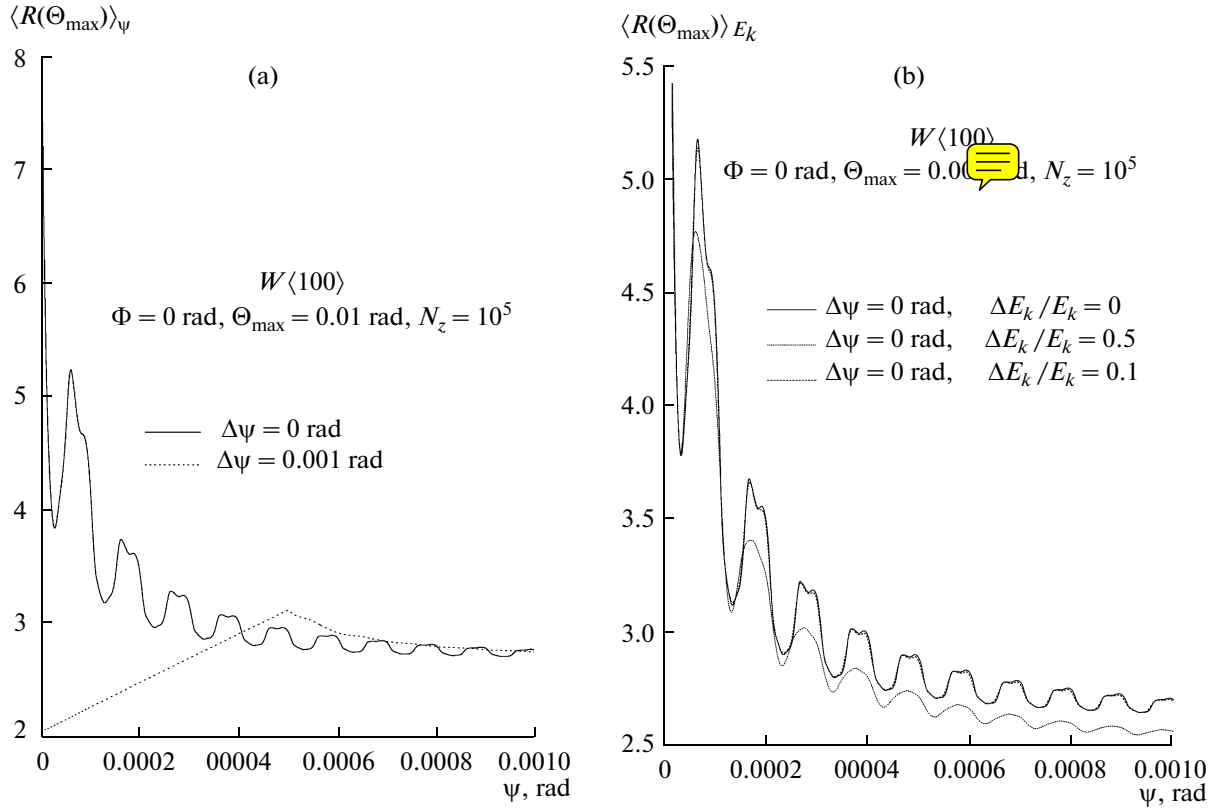

Fig. 5. The dependence of the relations $\langle R(\Theta_{max})\rangle_{\Psi}$ and $\langle R(\Theta_{max})\rangle_{E_k}$ (b) on the neutron entry angle Ψ relative to the crystal axis ⟨100⟩; the angle is $\Phi = 0$. The collimation angle is $\Theta_{max} = 0.01$ rad. The angular dispersion $\Delta\psi = 0.001$ rad (dashed line) is taken into account (dashed line); the results excluding the dispersion are shown by the solid line (a). The energy dispersion is taken into account: $\Delta E_k/E_k = 0.1$ is shown by dashes; $\Delta E_k/E_k = 0.5$ is shown by the dashed line; excluding the dispersion is shown by the solid line (b). The other parameters are similar to Fig. 2.

caused by the electromagnetic and nuclear scattering interference. Preliminary results of this study were published in [12].

ACKNOWLEDGMENTS

The work was partially supported by a grant from the Federal Agency on Science and Innovations, state contract no. 02.740.11.0238; a grant for support of leading scientific schools, project no. 3558.2010.2; and a grant from the Russian Foundation for Basic Research no. 10-02-01386-a.

REFERENCES

1. M. L. Ter-Mikaelyan, *Influence of the Medium on Electromagnetic Processes at High Energies* (Akad. Nauk Arm.SSR, Yerevan, 1969) [in Russian].
2. V. N. Baier, V. M. Katkov, and V. M. Strakhovenko, *Electromagnetic Processes at High Energy in Oriented Monocrystals* (Nauka, Novosibirsk, 1989) [in Russian].
3. J. Schwinger, Phys. Rev. **73**, 407 (1948).
4. Yu. A. Aleksandrov and I. I. Bondarenko, Sov. Phys. JETP **4**, 612 (1956).
5. Yu. A. Alexandrov, Preprint No. E3-2006-142 (JINR, Dubna, 2006).
6. A. S. Dyumin, I. Ya. Korenblit, V. A. Ruban, and B. B. Tokarev, JETP Lett. **31**, 384 (1980).
7. V. G. Baryshevskii and A. M. Zaitseva, Izv. Vyssh. Uchebn. Zaved., Fiz., No. 3, 103 (1985).
8. A. S. Dyumin, V. A. Ruban, B. B. Tokarev, and M. F. Vlasov, JETP Lett. **42**, 71 (1985).
9. Yu. P. Kunashenko and Yu. L. Pivovarov, in *Proceedings of the 51st Workshop of the INFN on Charged and Neutral Particles Channeling Phenomena, Channeling 2008, Eloisatron Project Erice, Italy, Oct. 25–Nov. 1, 2008* (World Scientific, Singapore, 2010), p. 794.
10. Yu. P. Kunashenko and Yu. L. Pivovarov, Nucl. Instrum. Methods Phys. Res. B **114**, 237 (1996).
11. Y. Okazaki, M. Andreyashkin, K. Chouffany, et al., Phys. Lett. A **271**, 110 (2000).
12. Yu. P. Kunashenko and Yu. L. Pivovarov, in *Proceedings of the 4th International Conference on Charged and Neutral Particles Channeling Phenomena, Channeling 2010, Ferrara, Italy, Oct. 3–8, 2010* (Univ. of Ferrara, Italy, 2010), p. 201.

SPELL: 1. ok